THE JOURNAL OF PHYSICAL CHEMISTRY Letters

Letter

Cite This: J. Phys. Chem. Lett. 2018, 9, 6779−6785

pubs.acs.org/JPCL

Using SERS To Understand the Binding of N-Heterocyclic Carbenes to Gold Surfaces

Michael J. Trujillo,[†] Shelby L. Strausser,[‡] Jeffrey C. Becca,[§] Joseph F. DeJesus,[‡] Lasse Jensen,*[,§] David M. Jenkins,*[,‡] and Jon P. Camden*[,†]

[†]Department of Chemistry and Biochemistry, University of Notre Dame, Notre Dame, Indiana 46556, United States

[‡]Department of Chemistry, University of Tennessee, Knoxville, Tennessee 37996, United States

[§]Department of Chemistry, The Pennsylvania State University, 104 Chemistry Building, University Park, Pennsylvania 16802-4615, United States

Supporting Information

ABSTRACT: Surface functionalization is an essential component of most applications of noble-metal surfaces. Thiols and amines are traditionally employed to attach molecules to noble-metal surfaces, but they have limitations. A growing body of research, however, suggests that N-heterocyclic carbenes (NHCs) can be readily employed for surface functionalization with superior chemical stability compared with thiols. We demonstrate the power of surface-enhanced Raman scattering combined with theory to present a comprehensive picture of NHC binding to gold surfaces. In particular, we synthesize a library of NHC isotopologues and use surface-enhanced Raman scattering to record the vibrational spectra of these NHCs while bound to gold surfaces. Our experimental data are compared with first-principles theory, yielding numerous new insights into the binding of NHCs to gold surfaces. In addition to these insights, we expect our approach to be a general method for probing the local surface properties of NHC-functionalized surfaces for their expanding use in sensing applications.

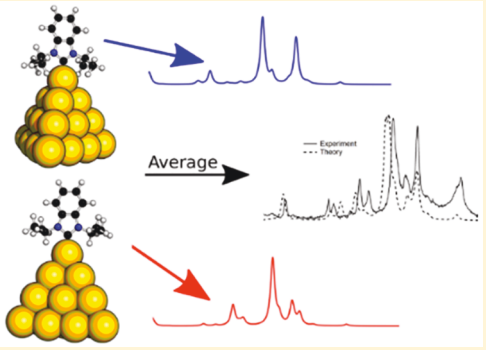

The role of surface functionalization cannot be underestimated when considering the myriad of applications of noble-metal surfaces. It plays a critical role in sensing,[1] drug delivery,[2] electronics,[3,4] surface protection,[5] and synthesis of uniquely shaped nanoparticles.[6] Amines and thiols are often the first choice when functionalization of gold surfaces is required because they have relatively high affinity for noble-metal surfaces, with binding energies of 25 and 125 kJ mol^{-1} to gold, respectively.[7,8] Whereas thiols, in particular, are used in many applications, their stability is greatly diminished in harsh chemical environments, such as oxidizing conditions, high temperature, and pH extremes.[9,10] A viable alternative to thiols for functionalized gold surfaces has remained elusive until the recent emergence of N-heterocyclic carbenes (NHCs).[11]

Although the binding of NHCs to gold surfaces is very strong, the free carbene is quite reactive[12] and their use was historically limited to carefully controlled chemical environments, which are often impractical for widespread adoption. Fortunately, progress has been made in the preparation of air-stable protected carbenes that serve as precursors to self-assembled monolayers on gold,[11,13,14] and NHC-functionalized gold films have been used in surface plasmon resonance[15,16] and electrochemical[11,17] measurements. Additionally, there is a growing body of literature reports on the preparation of NHC-functionalized nanoparticles.[18−24] After the initial reports of NHC-functionalized gold surfaces, the NHC binding, stability, and monolayer formation have been interrogated by a variety of methods.[11,13,25,26]

Whereas we recently demonstrated the first application of NHCs for SERS and showed that their robust binding allows postsynthetic modifications,[27] fundamental questions relating to the binding of NHCs to gold surfaces remain unexplored: (1) Where do NHCs prefer to bind on gold surfaces, (2) are the vibrational modes of surface-bound species sensitive to the NHC side moieties, and (3) which vibrational modes contribute most strongly to the SERS spectrum (Figure 1)? SERS is uniquely positioned to answer these questions because it possesses extreme sensitivity and an ability to measure the vibrational fingerprint of species in close proximity to plasmonic metal nanostructures without employing high-vacuum or complicated experimental setups. SERS can determine adsorbate orientation,[28−30] and detailed vibrational mode assignments can be made by deuteration of adsorbate molecules[31] and comparison with first-principles theory.[32,33] Deuteration of surface-bound species alters both the molecular motions and vibrational mode energies while minimally altering other properties such as the affinity for the metal surface, a feature that was exploited when measuring single-molecule SERS spectra.[34−37] As such, it provides an excellent vehicle for exploring the detailed surface vibrational spectroscopy of NHC monolayers on noble metals.

Received: September 7, 2018
Accepted: October 23, 2018
Published: October 23, 2018

DOI: 10.1021/acs.jpclett.8b02764
J. Phys. Chem. Lett. 2018, 9, 6779−6785

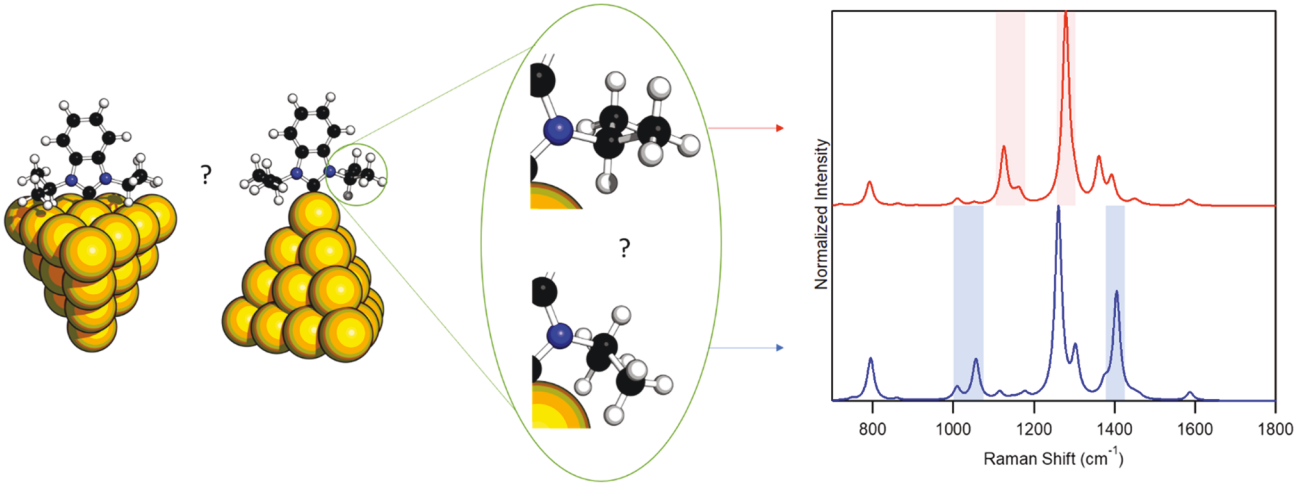

Figure 1. In this Letter, we investigate preferred binding of NHCs to gold surfaces: (1) surface versus tip (left), (2) the influence of side groups and their orientation (middle), and (3) which modes contribute the greatest SERS signal (right).

In this Letter, we synthesize an NHC library composed of deuterated isotopologues of the imidazolium and benzimidazolium NHCs. Using this library, we prepare NHC-functionalized, SERS-active gold surfaces for spectroscopic characterization. The resulting SERS spectra show excellent agreement with first-principles theory, allowing us to extract details of the surface binding motifs. Additionally, the spectroscopy of these compounds is carefully characterized with NMR, IR, Raman, and mass spectrometry. Using these data, we obtain a comprehensive picture of NHC binding to SERS-active gold substrates, and, more specifically, we obtain insight into several important open questions related to NHC films. More importantly, we demonstrate SERS to be a powerful tool when exploring as-yet unmade NHC-functionalized surfaces.

Synthesis of NHC−CO_2 Adducts and Surface Binding. In selecting the target NHCs for this study, it is notable that the N-substituent can affect the binding to the metal surface. Whereas multiple N-substituents, including methyl[20,38,39] and isopropyl[11] groups, have been studied, we selected isopropyls because they have been demonstrated to have excellent stability on gold.[13,27] The six target molecules in Figure 2

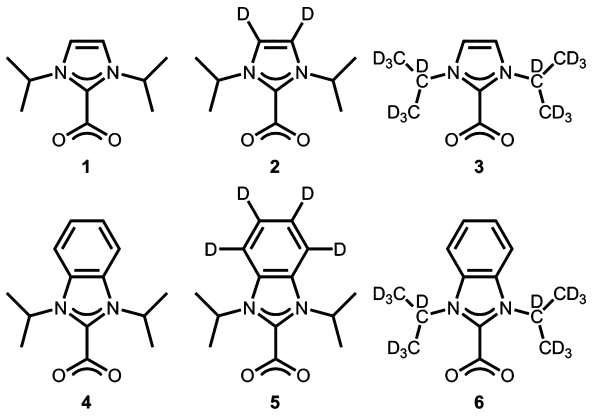

Figure 2. Isotopic variants of the imidazole (**1**−**3**) and benzimidazole (**4**−**6**) N-heterocyclic carbenes synthesized and spectroscopically characterized in this study.

require a synthetic strategy that allows for deuteration, followed by the formation of the NHC−CO_2 adduct. The NHC binds to gold following the loss of CO_2 under vacuum. In addition, upon exposure to air, the NHC−CO_2 adducts yield NHC−bicarbonate salts that are equally effective for gold binding.

For the imidazoliums, **1**−**3**, we followed the method of Louie for forming the final CO_2-adducted species.[40] The general schemes for their synthesis are shown in the SI. Compounds **2** and **3** required deuterium incorporation at >95% for quality SERS spectra because incomplete deuteration alters the symmetry of the molecule. In the case of **2**, very similar imidazoliums have been previously prepared by Bartsch.[41] Compound **3** can be deuterated with the addition of 2-bromopropane-d_7 (98+% d) to imidazole.

The synthesis of the benzimidazole versions of the CO_2 adducts, **4**−**6**, proved more challenging. Despite our recent report[27] of **4** via a synthetic approach that we employed for **1**−**3**, we subsequently discovered that it is a mixture of **4** and the bicarbonate salt (**4**·H_2O). This mixture for benzimidazole−CO_2 adduct and its associated bicarbonate salt is not uncommon because the pure CO_2 adducts of benzimidazolium are highly unstable (vide infra).[42] Fortuitously, Limbach previously prepared 2-carboxy-1,3-dimethyl-benzimidazolium, which differs only in the substituents off the nitrogen atoms.[43] Employing KO^{t}Bu as the base in THF with **10**, followed by CO_2 gas, yields the pure product 2-carboxy-1,3-diisopropyl-benzimidazolium, **4**, based on ^{13}C NMR in CD_2Cl_2 (Scheme S2 and Figure S12), which was consistent with Limbach's report.[43] In particular, the CO_2 peak at 156.21 ppm in CD_2Cl_2 is consistent with his value for 2-carboxy-1,3-dimethyl-benzimidazolium, which comes at 154.7 ppm and is distinct from the bicarbonate salt (vide infra).

Inserting deuterium into the benzimidazole ring was not as straightforward as the equivalent imidazole, but a series of four reactions led to **5**, which is deuterated on the aryl ring (Scheme S2). Deuteration proceeded via a modified procedure from Sajiki to give 97% total deuterium incorporation.[44] The benzimidazole, (4,5,6,7-d_4)-benzimidazole was formed through the addition of ethyl orthoformate to **11** under acidic conditions similar to the method of Bielawski.[45] Further reactions to form **5** proceeded in the same manner as for **4**. Finally, 2-carboxy-1,3-(d_{14})-diisopropylbenzimidazolium, **6**, was synthesized in two steps that were analogous to the reactions for the preparation of **3**. Deuterium incorporation for **6** is 99% on the isopropyl positions. The NHC−CO_2 adducts are

DOI: 10.1021/acs.jpclett.8b02764
J. Phys. Chem. Lett. 2018, 9, 6779−6785

important because they provide masked carbenes that are easily bound to the gold surface under atmospheric conditions without the need for special storage once they have been synthesized. We previously reported that **4** could be placed on AuFONs under solvent-free conditions by applying vacuum (5 Torr) at 120 °C.[27] However, the stability of the NHC−CO_2 adducts was tested to determine if they are effective after exposure to air. We investigated one imidazole NHC−CO_2 adduct, **2**, and one benzimidazole NHC−CO_2 adduct, **4**, for stability and effectiveness after air exposure (Scheme 1).

Scheme 1. Preparation of NHC AuFONs Either with or without Air Exposure

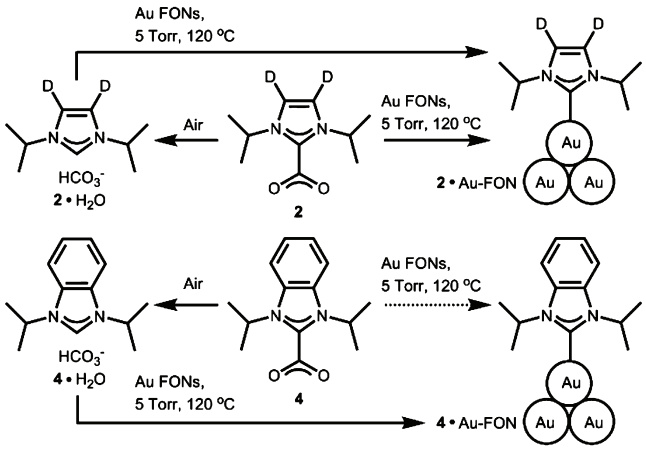

After exposure to air, the solids were dissolved in dry CD_2Cl_2 to evaluate their NMR spectra for decomposition. Compound **2** formed a nearly 50:50 mixture of **2** and its associated bicarbonate salt, **2**·H_2O, after 1 week of exposure, which is consistent with Taton's studies on similar NHCs (Scheme 1, top; Figure S49).[42] The key additional peaks in the ^{1}H NMR include the imidazolium peak at 10.97 ppm and the second set of peaks related to the isopropyl groups at 4.88 and 1.58 ppm. Conversely, tests with the benzimidazolium version showed that the decomposition to the bicarbonate salt was extremely rapid. The addition of air to **4** was tested at 4 days, 10 min, and 30 s (Scheme 1, bottom). In the first two cases, **4** was completely degraded to its bicarbonate salt **4**·H_2O (Figure S50). In the benzimidazolium case (**4**), there is a peak at 11.58 ppm and the isopropyl peaks shift upfield at 5.09 ppm, analogous to the imidazolium case. Only on the very short time of 30 s of air exposure were we able to observe both **4** and **4**·H_2O (Figure S52).

We deposited the NHCs on AuFONs because they are easy to prepare and are widely used for SERS studies.[46] AuFONs are gold film over nanosphere substrates prepared by the evaporation of gold (200 nm) on polystyrene nanospheres (600 nm diameter) using a chromium (5 nm) adhesion layer (see the SI for details).[47] Because the AuFONs were functionalized with the NHCs by placing a 1 to 2 mg amount of solid NHC precursor directly onto the AuFON then heating the AuFONs to 120 °C under vacuum (5 Torr), this suggests that the formation of the Au−NHC bond is equally possible from both the NHC−CO_2^- and the bicarbonate salt. In practice, the imidazole variants **1**−**3** primarily proceed from the direct CO_2 adduct, whereas the benzimidazole versions proceed through the bicarbonate salt (Scheme 1). This result is consistent with previous reports of Au-NHCs by Crudden, who employed the bicarbonate salts, and Glorius and Johnson, who directly used the CO_2 adducts for gold films.[13,14,26]

Analysis of SERS Spectra. Figure 3 displays a portion of the Raman spectrum of the protected carbene, the Raman

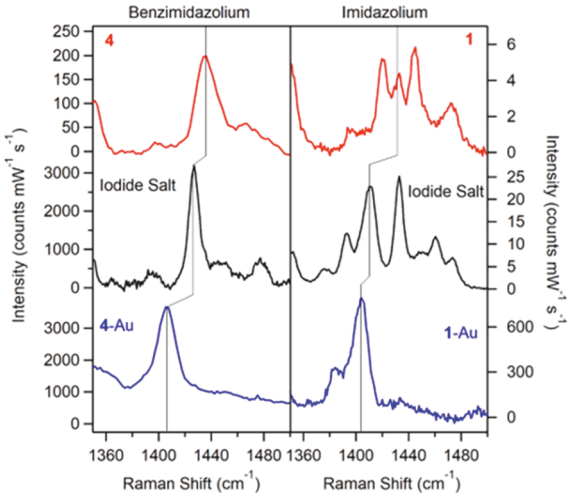

Figure 3. Left: Raman spectrum of the CO_2 adduct (red) and the benzimidazolium iodide precursor (black) of compound **4** compared with the surface-enhanced Raman spectrum of **4**-**Au** on the AuFON surface. Right: Raman spectrum of the CO_2 adduct (red) and the imidazolium iodide precursor (black) of compound **1** compared with the SERS spectrum of **1**-**Au** (blue). A clear red shift of the C−N bonds moving from the CO_2 adduct to the precursor and finally to the carbene, most evident in the benzimidazolium spectra and indicated by dotted line, is attributed to the change from an electron-withdrawing group (carboxylate), to a neutral molecule, and lastly an electron-donating group (gold surface).

spectrum of the iodide precursor, and the SERS spectrum of the carbene on an AuFON for the benzimidazolium and imidazolium families of compounds. The complete spectra can be found in the SI. A comparison of the Raman spectrum of the protected carbenes (**1**, **4**) to the SERS spectrum of the carbenes on gold (**1**-**Au**, **4**-**Au**) shows a 30 cm^{-1} red shift of the 1434 (**1**) and 1436 cm^{-1} (**4**) modes upon binding. The red shift of these bands is consistent with NHC binding to gold, which is electron-donating when compared with the electron-withdrawing nature of the CO_2 group. This interpretation is further supported by the Raman spectrum of the iodide precursor, which is expected to be intermediate between the Au-bound and the CO_2-protected NHC. Indeed, the Raman spectra of the iodide precursors display bands in between the two extremes at 1426 and 1410 cm^{-1} for the benzimidazolium and imidazolium iodide compounds, respectively. The theoretical data also capture this effect, predicting a ∼30 cm^{-1} red shift of vibrational modes upon the release of the CO_2 and binding to the AuFONs, in good agreement with experiment. Complete spectra and a pictorial representation of the vibrational modes of **4** and **1** are given in the SI (Figures S53 and S54, respectively).

Figure 4 displays the optimized geometry of compound **4** bound to the "tip" or the "surface" of a Au_{20} cluster. This cluster was chosen because it is known to be a good model for the calculation of SERS spectra.[48,49] The computational data suggest that both the tip and surface configurations are remarkably similar because the surface Au is distorted by the carbene, creating its own "tip," resembling an adatom. The theoretical calculations further demonstrate sensitivity to the geometry of

DOI: 10.1021/acs.jpclett.8b02764
J. Phys. Chem. Lett. 2018, 9, 6779−6785

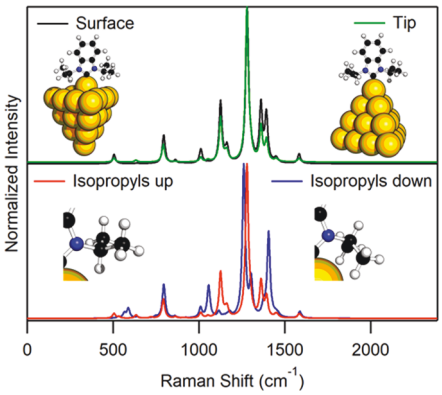

Figure 4. Top: Calculated SERS spectra of **4-Au** with the NHC bound to a "surface" gold atom (black) and a "tip" gold atom (green) of a Au_{20} cluster. Optimized geometries of both tip and surface cases are presented as inset images. The strength of the Au−C bond is sufficient to pull a gold atom up from the cluster despite the known stability of the Au_{20} surface. Bottom: Calculated SERS spectra of **4-Au** with isopropyl groups oriented up (red) and down (blue). The prominent differences between the spectra resulting from up and down isopropyl groups indicate that the SERS is very sensitive to the orientation of the side groups.

the R groups attached to the N, particularly for compound **4** (Figure 4, bottom). The best agreement between theory and experiment was obtained from an equal combination of upward and downward orientation of the isopropyl groups, as determined by creating a series of spectra ranging from 100% upward to 100% downward and calculating the correlation with the experimental data. A maximum correlation was obtained at 49% upward- and 51% downward-oriented isopropyl groups (Figure S55). The difference in energy between the two configurations is negligible for the level of theory used (4.59 and 3.75 kcal/mol difference for **4-Au** and **1-Au**, respectively), further supporting this view. The simulated Raman cross-sections for both the upward and downward configurations are also within the same order of magnitude, justifying the comparison between the individually normalized configurations.

The theoretical data also show that a surface gold atom is pulled up from the surface, which is remarkable given the inherent stability of the Au_{20} cluster used in the modeling.[50] This finding is in agreement with Glorius and Fuchs and coworkers' previously published scanning tunneling microscopy (STM) studies indicating that the carbene draws a gold atom from the surface, taking an adatom configuration, which can then move across the surface in this configuration by a "ballbot" type motion.[26] Taking these results together, the following discussion relies on calculations with the NHCs bound to the tip of a Au_{20} cluster with equal contribution from both the up and down isopropyl configurations.

Comparisons of experiment and theory for **1-Au** and **4-Au** (Figure 5) indicate that the most intense modes in the SERS spectra are due to the movement of the hydrogen atoms of the isopropyl groups bound to the NHC nitrogens, particularly the hydrogen bound to the central carbon of the isopropyl group. Modes listed in red and blue correspond to those that are primarily attributed to the up and down configured isopropyl groups, respectively. The high intensity of the modes centered on the isopropyl groups is logical because the isopropyl groups are closest to the surface, therefore benefiting from the greatest surface enhancement. Even though this interpretation appears sound, it is somewhat counterintuitive because in previous SERS spectra of aromatic molecules the most intense bands are dominated by modes centered on the ring.[51] Excellent agreement between the theory and experiment shown in Figure 5 also elucidates another key point. The experimental data are very accurately simulated with just two configurations averaged together in a near-1:1 ratio, showing that the distribution on the surface must contain primarily upward and downward isopropyl configurations. If other configurations were present in significant numbers on the surface, then the theory would need to include all possible configurations, considering the large effect the isopropyl groups have on the SERS spectra.

Figure 6 compares the experimental and predicted SERS spectra of NHCs where the hydrogens of the heterocycles have been substituted with deuterium, which allows us to further confirm our vibrational assignments. In this case, we additionally see modes that correspond to motion of the atoms in the heterocycle, although they are not the most intense bands in the spectrum. There is an obvious shift and change of intensity of the 1532 cm^{-1} mode in the SERS spectrum of **1-Au** after deuteration (**2-Au**), which is expected because that mode is dominated almost entirely by the motion of the ring hydrogens (Figure 6, left). A similar change is observed in the SERS spectra of **4-Au** and **5-Au**, notably from 807, 1129, and 1589 cm^{-1} to 817, 1123, and 1562 cm^{-1}, respectively (Figure 6, right).

The sensitivity of the isopropyl vibrations to the local geometry can be explored by deuterating the isopropyl wing groups instead of the ring protons. This change in weight is expected to greatly alter the resulting SERS spectra because the most intense modes of the protonated NHCs exhibit motion of the isopropyl group hydrogens, as discussed previously. Figure S56 displays the experimental SERS spectra of the NHCs with deuterated isopropyl groups (**3-Au** and **6-Au**). Surprisingly,

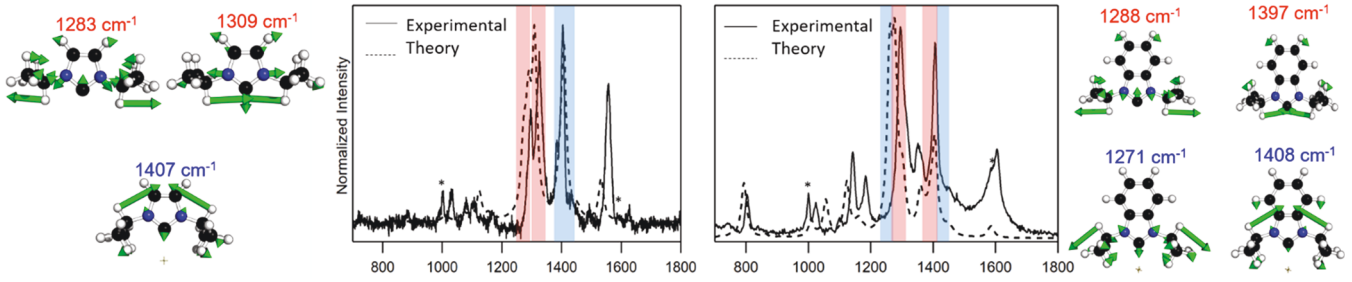

Figure 5. Experimental SERS spectra (solid) and theoretical SERS spectra (dashed), overlaid, show excellent agreement for both **1-Au** and **4-Au** (left and right, respectively). Theory shows that many of the most intense modes in the spectra are derived from motion on the isopropyl side groups. These modes are shown pictorially above the spectra with their energies. Red and blue coloring is used to indicate modes arising primarily from up- and down-oriented isopropyl groups, respectively. Asterisks indicate modes from polystyrene spheres below the gold film.

DOI: 10.1021/acs.jpclett.8b02764
J. Phys. Chem. Lett. 2018, 9, 6779−6785

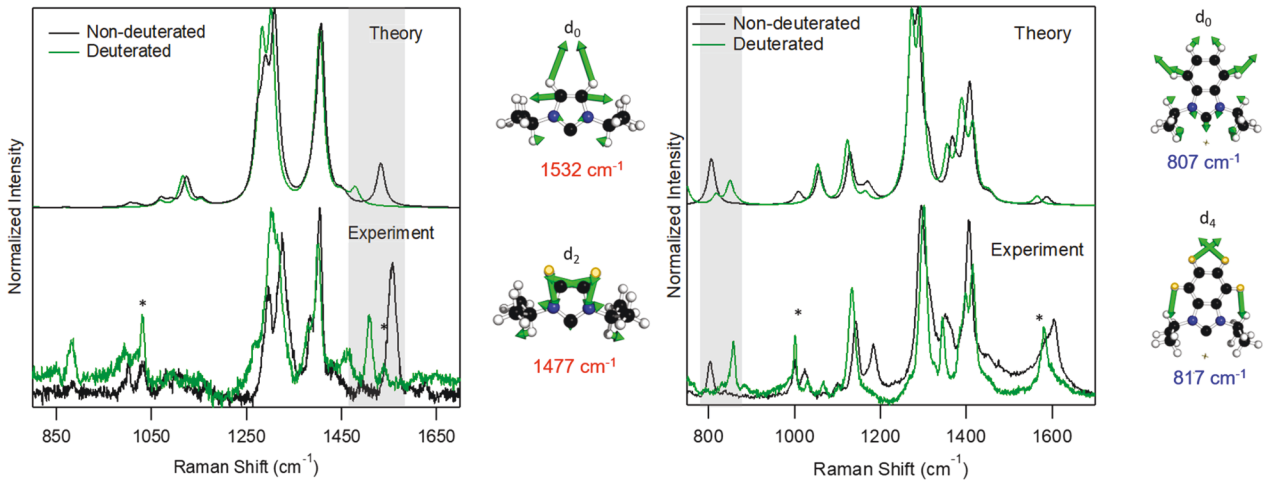

Figure 6. Left: Theoretical (top) and experimental (bottom) SERS spectra of **1-Au** (black) and **2-Au** (green). Right: Theoretical (top) and experimental (bottom) SERS spectra of **4-Au** (black) and **5-Au** (green). The isotope shifts upon deuteration are well reproduced by the theory, and several of the most perturbed modes are presented pictorially next to the spectra. * indicates a contribution from polystyrene spheres below the gold film.

the SERS spectra of the imidazolium and benzimidazolium carbenes with deuterated isopropyl wing groups become very similar to each other and are dominated by bands at 1352 or 1367 cm^{-1} in **3-Au** and **6-Au**, respectively. Clearly, deuteration of the isopropyl groups decouples the motion on the ring from the alkyl groups, which greatly increases the contribution of the imidazolium ring in the SERS spectra. Because both NHCs contain the imidazole ring, the resulting SERS spectra appear very similar. Additionally, two bands near 1000−1030 cm^{-1} are also present in both spectra and arise from motion on the isopropyl groups. The previously discussed ring modes near 1330−1340 cm^{-1} in the deuterated samples are visualized with vector representations in Figure S56. Figures S57−S59 present a detailed assignment of modes from the SERS spectra of **1-Au** to **6-Au**, followed by their pictorial representations.

Vector overlap of normal modes was calculated to elucidate the effect of deuteration on the isopropyl groups. This was done by calculating the difference in 3-N normal mode vectors between two pairs, the benzimidazolium (**4-Au** and **6-Au**) and the imidazolium (**1-Au** and **3-Au**). If the normal modes are mostly the same after deuteration, then a high vector overlap of normal modes would be expected. Results showed that for the **1-Au** to **3-Au** deuteration a significant decoupling occurred, with most of the intense modes for **1-Au** being heavily altered. The largest normal mode overlap for the 1407 cm^{-1} mode in **3-Au** was very small (~39% overlap). For the **4-Au** modes around 1408 cm^{-1}, a similar result was found but with slightly higher overlap (~53%). Modes that were not heavily related to the isopropyl groups, such as the 1532 cm^{-1} mode for **1-Au**, were found to have high mode overlaps (87%). This large difference in vector overlap for normal modes with isopropyl contribution further emphasizes how important the N-substituents are to the SERS spectra. Deuteration of the side groups largely decoupled ring and side group vibrations, which resulted in very different spectra.

In summary, in this manuscript, we presented a comprehensive experimental and theoretical investigation of the Raman and SERS spectra of benzimidazolium and imidazolium NHC-functionalized gold films by comparison of deuterated isotopologues of **1** and **4**. The NHC−Au films can be facilely formed from either the NHC−CO_2 adducts or the NHC−bicarbonate salt, which is a degradation product of the NHC−CO_2 adduct from exposure to air. The fidelity of the match between the theoretical and the experimental SERS spectra of the NHCs on the gold surfaces yields three major findings. First, the NHCs binds to tips and adatoms on the film and not a purely flat surface. Second, the isopropyl moieties on the NHCs point to a mixture of solely up and down toward the gold surface, and it is impossible to replicate the experimental spectra with only one isopropyl position. Finally, the vibrational modes in the spectra are dominated by the hydrogens on the isopropyl moieties and not the ring modes of the NHC. Whereas this is due to the close proximity of these hydrogen atoms to the surface plasmon, this phenomenon is not typically observed with other typical binding ligands, such as amines or thiols, because their modes cannot be easily separated from a ring mode itself. Our method provides a general method for understanding the surface structure of NHCs films, which is critical when targeting NHCs with specific properties on gold surfaces.

■ ASSOCIATED CONTENT

Supporting Information

The Supporting Information is available free of charge on the ACS Publications website at DOI: 10.1021/acs.jpclett.8b02764.

Supplementary crystallographic information (CIF)
Synthesis and characterization of all described compounds as well as additional SERS and theory data (PDF)

■ AUTHOR INFORMATION

Corresponding Authors

*J.P.C.: E-mail: jon.camden@nd.edu.
*D.M.J.: E-mail: jenkins@ion.chem.utk.edu.
*L.J.: E-mail: jensen@chem.psu.edu.

ORCID

Michael J. Trujillo: 0000-0003-3134-6285
Lasse Jensen: 0000-0003-1237-5021
David M. Jenkins: 0000-0003-2683-9157
Jon P. Camden: 0000-0002-6179-2692

Author Contributions

The manuscript was written through contributions of all authors. All authors have given approval to the final version of the manuscript.

DOI: 10.1021/acs.jpclett.8b02764
J. Phys. Chem. Lett. 2018, 9, 6779−6785

Notes

The authors declare no competing financial interest.

■ ACKNOWLEDGMENTS

This material is based on work supported by the National Science Foundation under grant numbers CHE-1709881, CHE-1709468, CHE-1362825, and NRT-1449785. Any opinions, findings, and conclusions or recommendations expressed in this material are those of the authors and do not necessarily reflect the views of the National Science Foundation. Portions of this work were conducted with Advanced Cyberinfrastructure computational resources provided by The Institute for Cyber-Science at The Pennsylvania State University (http://ics.psu.edu).

■ ABBREVIATIONS

SERS, surface-enhanced Raman scattering; AuFON, gold film over nanosphere; NHC, N-heterocyclic carbene

■ REFERENCES

(1) Homola, J. Present and Future of Surface Plasmon Resonance Biosensors. *Anal. Bioanal. Chem.* **2003**, *377*, 528−539.
(2) Han, G.; Ghosh, P.; Rotello, V. M. Functionalized Gold Nanoparticles for Drug Delivery. *Nanomedicine* **2007**, *2*, 113−123.
(3) DiBenedetto, S. A.; Facchetti, A.; Ratner, M. A.; Marks, T. J. Molecular Self-Assembled Monolayers and Multilayers for Organic and Unconventional Inorganic Thin-Film Transistor Applications. *Adv. Mater.* **2009**, *21*, 1407−1433.
(4) Lv, A.; Freitag, M.; Chepiga, K. M.; Schäfer, A. H.; Glorius, F.; Chi, L. N-Heterocyclic-Carbene-Treated Gold Surfaces in Pentacene Organic Field-Effect Transistors: Improved Stability and Contact at the Interface. *Angew. Chem., Int. Ed.* **2018**, *57*, 4792−4796.
(5) Zamborini, F. P.; Crooks, R. M. Corrosion Passivation of Gold by N-Alkanethiol Self-Assembled Monolayers: Effect of Chain Length and End Group. *Langmuir* **1998**, *14*, 3279−3286.
(6) Grzelczak, M.; Pérez-Juste, J.; Mulvaney, P.; Liz-Marzán, L. M. Shape Control in Gold Nanoparticle Synthesis. *Chem. Soc. Rev.* **2008**, *37*, 1783−1791.
(7) Hoft, R. C.; Ford, M. J.; McDonagh, A. M.; Cortie, M. B. Adsorption of Amine Compounds on the Au(111) Surface: A Density Functional Study. *J. Phys. Chem. C* **2007**, *111*, 13886−13891.
(8) Lavrich, D. J.; Wetterer, S. M.; Bernasek, S. L.; Scoles, G. Physisorption and Chemisorption of Alkanethiols and Alkyl Sulfides on Au(111). *J. Phys. Chem. B* **1998**, *102*, 3456−3465.
(9) Srisombat, L.; Jamison, A. C.; Lee, T. R. Stability: A Key Issue for Self-Assembled Monolayers on Gold as Thin-Film Coatings and Nanoparticle Protectants. *Colloids Surf., A* **2011**, *390*, 1−19.
(10) Vericat, C.; Vela, M. E.; Benitez, G.; Carro, P.; Salvarezza, R. C. Self-Assembled Monolayers of Thiols and Dithiols on Gold: New Challenges for a Well-Known System. *Chem. Soc. Rev.* **2010**, *39*, 1805−1834.
(11) Crudden, C. M.; Horton, J. H.; Ebralidze, I. I.; Zenkina, O. V.; McLean, A. B.; Drevniok, B.; She, Z.; Kraatz, H.-B.; Mosey, N. J.; Seki, T.; Keske, E. C.; Leake, J. D.; Rousina-Webb, A.; Wu, G. Ultra Stable Self-Assembled Monolayers of N-Heterocyclic Carbenes on Gold. *Nat. Chem.* **2014**, *6*, 409−414.
(12) Hopkinson, M. N.; Richter, C.; Schedler, M.; Glorius, F. An Overview of N-Heterocyclic Carbenes. *Nature* **2014**, *510*, 485−496.
(13) Crudden, C. M.; Horton, J. H.; Narouz, M. R.; Li, Z.; Smith, C. A.; Munro, K.; Baddeley, C. J.; Larrea, C. R.; Drevniok, B.; Thanabalasingam, B.; McLean, A. B.; Zenkina, O. V.; Ebralidze, I. I.; She, Z.; Kraatz, H.-B.; Mosey, N. J.; Saunders, L. N.; Yagi, A. Simple Direct Formation of Self-Assembled N-Heterocyclic Carbene Monolayers on Gold and Their Application in Biosensing. *Nat. Commun.* **2016**, *7*, 12654.
(14) Zhukhovitskiy, A. V.; Mavros, M. G.; Van Voorhis, T.; Johnson, J. A. Addressable Carbene Anchors for Gold Surfaces. *J. Am. Chem. Soc.* **2013**, *135*, 7418−7421.
(15) Li, Z.; Munro, K.; Ebralize, I. I.; Narouz, M. R.; Padmos, J. D.; Hao, H.; Crudden, C. M.; Horton, J. H. N-Heterocyclic Carbene Self-Assembled Monolayers on Gold as Surface Plasmon Resonance Biosensors. *Langmuir* **2017**, *33*, 13936−13944.
(16) Li, Z.; Narouz, M. R.; Munro, K.; Hao, B.; Crudden, C. M.; Horton, J. H.; Hao, H. Carboxymethylated Dextran-Modified N-Heterocyclic Carbene Self-Assembled Monolayers on Gold for Use in Surface Plasmon Resonance Biosensing. *ACS Appl. Mater. Interfaces* **2017**, *9*, 39223−39234.
(17) Cao, Z.; Derrick, J. S.; Xu, J.; Gao, R.; Gong, M.; Nichols, E. M.; Smith, P. T.; Liu, X.; Wen, X.; Copéret, C.; Chang, C. J. Chelating N-Heterocyclic Carbene Ligands Enable Tuning of Electrocatalytic CO_2 Reduction to Formate and Carbon Monoxide: Surface Organometallic Chemistry. *Angew. Chem., Int. Ed.* **2018**, *57*, 4981−4985.
(18) Baquero, E. A.; Tricard, S.; Coppel, Y.; Flores, J. C.; Chaudret, B.; de Jesús, E. Water-Soluble Platinum Nanoparticles Stabilized by Sulfonated N-Heterocyclic Carbenes: Influence of the Synthetic Approach. *Dalton Trans* **2018**, *47*, 4093−4104.
(19) Bridonneau, N.; Hippolyte, L.; Mercier, D.; Portehault, D.; Desage-El Murr, M.; Marcus, P.; Fensterbank, L.; Chanéac, C.; Ribot, F. N-Heterocyclic Carbene-Stabilized Gold Nanoparticles with Tunable Sizes. *Dalton Trans* **2018**, *47*, 6850−6859.
(20) MacLeod, M. J.; Johnson, J. A. Pegylated N-Heterocyclic Carbene Anchors Designed to Stabilize Gold Nanoparticles in Biologically Relevant Media. *J. Am. Chem. Soc.* **2015**, *137*, 7974−7977.
(21) Man, R. W. Y.; Li, C.-H.; MacLean, M. W. A.; Zenkina, O. V.; Zamora, M. T.; Saunders, L. N.; Rousina-Webb, A.; Nambo, M.; Crudden, C. M. Ultrastable Gold Nanoparticles Modified by Bidentate N-Heterocyclic Carbene Ligands. *J. Am. Chem. Soc.* **2018**, *140*, 1576−1579.
(22) Narouz, M. R.; Li, C.-H.; Nazemi, A.; Crudden, C. M. Amphiphilic N-Heterocyclic Carbene-Stabilized Gold Nanoparticles and Their Self-Assembly in Polar Solvents. *Langmuir* **2017**, *33*, 14211−14219.
(23) Salorinne, K.; Man, R. W. Y.; Li, C.-H.; Taki, M.; Nambo, M.; Crudden, C. M. Water-Soluble N-Heterocyclic Carbene-Protected Gold Nanoparticles: Size-Controlled Synthesis, Stability, and Optical Properties. *Angew. Chem., Int. Ed.* **2017**, *56*, 6198−6202.
(24) Vignolle, J.; Tilley, T. D. N-Heterocyclic Carbene-Stabilized Gold Nanoparticles and Their Assembly into 3D Superlattices. *Chem. Commun.* **2009**, 7230−7232.
(25) Larrea, C. R.; Baddeley, C. J.; Narouz, M. R.; Mosey, N. J.; Horton, J. H.; Crudden, C. M. N-Heterocyclic Carbene Self-Assembled Monolayers on Copper and Gold: Dramatic Effect of Wingtip Groups on Binding, Orientation and Assembly. *ChemPhysChem* **2017**, *18*, 3536−3539.
(26) Wang, G.; Rühling, A.; Amirjalayer, S.; Knor, M.; Ernst, J. B.; Richter, C.; Gao, H.-J.; Timmer, A.; Gao, H.-Y.; Doltsinis, N. L.; Glorius, F.; Fuchs, H. Ballbot-Type Motion of N-Heterocyclic Carbenes on Gold Surfaces. *Nat. Chem.* **2017**, *9*, 152.
(27) DeJesus, J. F.; Trujillo, M. J.; Camden, J. P.; Jenkins, D. M. N-Heterocyclic Carbenes as a Robust Platform for Surface-Enhanced Raman Spectroscopy. *J. Am. Chem. Soc.* **2018**, *140*, 1247−1250.
(28) Allen, C. S.; Van Duyne, R. P. Orientational Specificity of Raman Scattering from Molecules Adsorbed on Silver Electrodes. *Chem. Phys. Lett.* **1979**, *63*, 455−459.
(29) Golab, J. T.; Sprague, J. R.; Carron, K. T.; Schatz, G. C.; Van Duyne, R. P. A Surface Enhanced Hyper-Raman Scattering Study of Pyridine Adsorbed onto Silver: Experiment and Theory. *J. Chem. Phys.* **1988**, *88*, 7942−7951.
(30) Turley, H. K.; Hu, Z.; Jensen, L.; Camden, J. P. Surface-Enhanced Resonance Hyper-Raman Scattering Elucidates the Molecular Orientation of Rhodamine 6g on Silver Colloids. *J. Phys. Chem. Lett.* **2017**, *8*, 1819−1823.
(31) Giese, B.; McNaughton, D. Surface-Enhanced Raman Spectroscopic and Density Functional Theory Study of Adenine Adsorption to Silver Surfaces. *J. Phys. Chem. B* **2002**, *106*, 101−112.

DOI: 10.1021/acs.jpclett.8b02764
J. Phys. Chem. Lett. 2018, 9, 6779−6785

(32) Chiang, N.; Jiang, N.; Madison, L. R.; Pozzi, E. A.; Wasielewski, M. R.; Ratner, M. A.; Hersam, M. C.; Seideman, T.; Schatz, G. C.; Van Duyne, R. P. Probing Intermolecular Vibrational Symmetry Breaking in Self-Assembled Monolayers with Ultrahigh Vacuum Tip-Enhanced Raman Spectroscopy. *J. Am. Chem. Soc.* **2017**, *139*, 18664−18669.
(33) Lee, J.; Tallarida, N.; Chen, X.; Jensen, L.; Apkarian, V. A. Microscopy with a Single-Molecule Scanning Electrometer. *Sci. Advances* **2018**, *4*, eaat5472.
(34) Blackie, E.; Le Ru, E. C.; Meyer, M.; Timmer, M.; Burkett, B.; Northcote, P.; Etchegoin, P. G. Bi-Analyte Sers with Isotopically Edited Dyes. *Phys. Chem. Chem. Phys.* **2008**, *10*, 4147−4153.
(35) Camden, J. P.; Dieringer, J. A.; Wang, Y.; Masiello, D. J.; Marks, L. D.; Schatz, G. C.; Van Duyne, R. P. Probing the Structure of Single-Molecule Surface-Enhanced Raman Scattering Hot Spots. *J. Am. Chem. Soc.* **2008**, *130*, 12616−12617.
(36) Kleinman, S. L.; Ringe, E.; Valley, N.; Wustholz, K. L.; Phillips, E.; Scheidt, K. A.; Schatz, G. C.; Van Duyne, R. P. Single-Molecule Surface-Enhanced Raman Spectroscopy of Crystal Violet Isotopologues: Theory and Experiment. *J. Am. Chem. Soc.* **2011**, *133*, 4115−4122.
(37) Titus, E. J.; Weber, M. L.; Stranahan, S. M.; Willets, K. A. Super-Resolution Sers Imaging Beyond the Single-Molecule Limit: An Isotope-Edited Approach. *Nano Lett.* **2012**, *12*, 5103−5110.
(38) Campos, J.; Sharninghausen, L. S.; Crabtree, R. H.; Balcells, D. A Carbene-Rich but Carbonyl-Poor $[Ir_6(Ime)_8(CO)_2H_{14}]^{2+}$ Polyhydride Cluster as a Deactivation Product from Catalytic Glycerol Dehydrogenation. *Angew. Chem., Int. Ed.* **2014**, *53*, 12808−12811.
(39) Voutchkova, A. M.; Appelhans, L. N.; Chianese, A. R.; Crabtree, R. H. Disubstituted Imidazolium-2-Carboxylates as Efficient Precursors to N-Heterocyclic Carbene Complexes of Rh, Ru, Ir, and Pd. *J. Am. Chem. Soc.* **2005**, *127*, 17624−17625.
(40) Van Ausdall, B. R.; Glass, J. L.; Wiggins, K. M.; Aarif, A. M.; Louie, J. A Systematic Investigation of Factors Influencing the Decarboxylation of Imidazolium Carboxylates. *J. Org. Chem.* **2009**, *74*, 7935−7942.
(41) Dzyuba, S. V.; Li, S.; Bartsch, R. A. Convenient Syntheses of Perdeuterated Ionic Liquids. *J. Heterocycl. Chem.* **2007**, *44*, 223−225.
(42) Fèvre, M.; Pinaud, J.; Leteneur, A.; Gnanou, Y.; Vignolle, J.; Taton, D.; Miqueu, K.; Sotiropoulos, J.-M. Imidazol(in)Ium Hydrogen Carbonates as a Genuine Source of N-Heterocyclic Carbenes (Nhcs): Applications to the Facile Preparation of Nhc Metal Complexes and to Nhc-Organocatalyzed Molecular and Macromolecular Syntheses. *J. Am. Chem. Soc.* **2012**, *134*, 6776−6784.
(43) Lindner, R.; Lejkowski, M. L.; Lavy, S.; Deglmann, P.; Wiss, K. T.; Zarbakhsh, S.; Meyer, L.; Limbach, M. Ring-Opening Polymerization and Copolymerization of Propylene Oxide Catalyzed by N-Heterocyclic Carbenes. *ChemCatChem* **2014**, *6*, 618−625.
(44) Ito, N.; Esaki, H.; Maesawa, T.; Imamiya, E.; Maegawa, T.; Sajiki, H. Efficient and Selective Pt/C-Catalyzed H−D Exchange Reaction of Aromatic Rings. *Bull. Chem. Soc. Jpn.* **2008**, *81*, 278−286.
(45) Khramov, D. M.; Bielawski, C. W. Donor−Acceptor Triazenes: Synthesis, Characterization, and Study of Their Electronic and Thermal Properties. *J. Org. Chem.* **2007**, *72*, 9407−9417.
(46) Farcau, C.; Astilean, S. Mapping the Sers Efficiency and Hot-Spots Localization on Gold Film over Nanospheres Substrates. *J. Phys. Chem. C* **2010**, *114*, 11717−11722.
(47) Péron, O.; Rinnert, E.; Toury, T.; Lamy de la Chapelle, M.; Compère, C. Quantitative Sers Sensors for Environmental Analysis of Naphthalene. *Analyst* **2011**, *136*, 1018−1022.
(48) Aikens, C. M.; Schatz, G. C. Tddft Studies of Absorption and Sers Spectra of Pyridine Interacting with Au_{20}. *J. Phys. Chem. A* **2006**, *110*, 13317−13324.
(49) Zhao, L.; Jensen, L.; Schatz, G. C. Pyridine−Ag_{20} Cluster: A Model System for Studying Surface-Enhanced Raman Scattering. *J. Am. Chem. Soc.* **2006**, *128*, 2911−2919.
(50) Li, J.; Li, X.; Zhai, H.-J.; Wang, L.-S. Au_{20}: A Tetrahedral Cluster. *Science* **2003**, *299*, 864−867.
(51) Watanabe, H.; Hayazawa, N.; Inouye, Y.; Kawata, S. Dft Vibrational Calculations of Rhodamine 6G Adsorbed on Silver: Analysis of Tip-Enhanced Raman Spectroscopy. *J. Phys. Chem. B* **2005**, *109*, 5012−5020.

DOI: 10.1021/acs.jpclett.8b02764
J. Phys. Chem. Lett. 2018, 9, 6779−6785